

## Article

# A Study on the Corrosion Characteristics of Internal Combustion Engine Materials in Second-Generation Jatropa Curcas Biodiesel

M. Shahabuddin <sup>1,6,\*</sup> , M. Mofijur <sup>2,3</sup> , Md. Bengir Ahmed Shuvho <sup>4</sup> , M. A. K. Chowdhury <sup>5</sup>, M. A. Kalam <sup>6</sup> , H. H. Masjuki <sup>6,7</sup> and M. A. Chowdhury <sup>8</sup> 

- <sup>1</sup> Carbon Technology Research Centre, School of Engineering, Information Technology and Physical Sciences, Federation University, P.O. Box 3191, Gippsland, VIC 3841, Australia
  - <sup>2</sup> Centre for Green Technology, Faculty of Engineering and Information Technology, University of Technology, Sydney, NSW 2007, Australia; MdMofijur.Rahman@uts.edu.au
  - <sup>3</sup> Department of Mechanical Engineering, Prince Mohammad Bin Fahd University, Al Khobar 31952, Saudi Arabia
  - <sup>4</sup> Department of Industrial and Production Engineering, National Institute of Textile Engineering and Research (NITER), Savar, Dhaka 1350, Bangladesh; bengir.ipe@niter.edu.bd
  - <sup>5</sup> Faculty of Science and Engineering, Southern Cross University, Lismore, NSW 2480, Australia; mohammad.chowdhury@scu.edu.au
  - <sup>6</sup> Centre for Energy Sciences, Faculty of Engineering, University of Malaya, Kuala Lumpur 50603, Malaysia; kalam@um.edu.my (M.A.K.); masjuki@iium.edu.my (H.H.M.)
  - <sup>7</sup> Department of Mechanical Engineering, Faculty of Engineering, IIUM, Kuala Lumpur 50728, Malaysia
  - <sup>8</sup> Department of Mechanical Engineering, Dhaka University of Engineering and Technology (DUET), Gazipur 1707, Bangladesh; asad@duet.ac.bd
- \* Correspondence: s.ahmmad@federation.edu.au



**Citation:** Shahabuddin, M.; Mofijur, M.; Shuvho, M.B.A.; Chowdhury, M.A.K.; Kalam, M.A.; Masjuki, H.H.; Chowdhury, M.A. A Study on the Corrosion Characteristics of Internal Combustion Engine Materials in Second-Generation Jatropa Curcas Biodiesel. *Energies* **2021**, *14*, 4352. <https://doi.org/10.3390/en14144352>

Academic Editor: Attilio Converti

Received: 5 June 2021  
Accepted: 13 July 2021  
Published: 19 July 2021

**Publisher's Note:** MDPI stays neutral with regard to jurisdictional claims in published maps and institutional affiliations.



**Copyright:** © 2021 by the authors. Licensee MDPI, Basel, Switzerland. This article is an open access article distributed under the terms and conditions of the Creative Commons Attribution (CC BY) license (<https://creativecommons.org/licenses/by/4.0/>).

**Abstract:** The corrosiveness of biodiesel affects the fuel processing infrastructure and different parts of an internal combustion (IC) engine. The present study investigates the corrosion behaviour of automotive materials such as stainless steel, aluminium, cast iron, and copper in 20% (B20) and 30% (B30) by volume second-generation Jatropa biodiesel using an immersion test. The results were compared with petro-diesel (B0). Various fuel properties such as the viscosity, density, water content, total acid number (TAN), and oxidation stability were investigated after the immersion test using ASTM D341, ASTM D975, ASTM D445, and ASTM D6751 standards. The morphology of the corroded materials was investigated using optical microscopy and scanning electron microscopy (SEM), whereas the elemental analysis was carried out using energy-dispersive X-ray spectroscopy (EDS). The highest corrosion using biodiesel was detected in copper, while the lowest was detected in stainless steel. Using B20, the rate of corrosion in copper and stainless steel was 17% and 14% higher than when using diesel, which further increased to 206% and 86% using B30. After the immersion test, the viscosity, water content, and TAN of biodiesel were increased markedly compared to petro-diesel.

**Keywords:** jatropa biodiesel; corrosion rate; automotive materials; morphology; immersion test

## 1. Introduction

The growing interest in biofuels research is due to its favourable physicochemical properties, including biodegradability, renewability, compatibility, non-toxicity, high cetane number, and environmentally friendliness [1,2]. Biodiesel is classified as first, second, and third generation based on its source of raw materials or feedstocks. The most widely investigated feedstock is based on edible oil, which is known as first-generation biodiesel [3]. However, it has been argued that the use of edible food crops for the production of first-generation biofuels effectively reduces the amount of edible food for human consumption, leading to an increase the food prices in the global food market [4]. Although first-generation biofuels help satisfy the human needs for fuel, at the same time, it takes

away some resources intended for more important human needs such as the needs for nourishment. Hence, using edible feedstock for biofuel has sparked the “food vs. fuel” debate more recently. This provides researchers with incentives to explore other sources for biofuels that do not disrupt the human’s food supply. The second-generation biodiesel eliminates the dependency on edible food crops for the production of fuel [5].

It has been reported that second-generation biodiesel can be considered as a substitute for fossil fuel for internal combustion (IC) engines [6]. In addition, there is no need for any modifications to the IC engine hardware. Usually, fuel is exposed to metallic and non-metallic elements in engine systems. Ferrous materials such as steel, cast iron, and non-ferrous materials such as aluminium and copper alloys are used in the fuel system [7]. Biodiesel being unsaturated fatty acid is reactive with metallic materials because of the oxidation reactions that occur while passing from the fuel tank to the combustion chamber. In addition, biodiesel promotes autoxidation and hygroscopicity with the presence of different materials, which cause biodiesel degradation and corrosiveness [8,9]. In addition, during use or storage, biodiesel experiences different processes, including moisture absorption and microorganisms attack and thus becomes corrosive further. Moreover, some impurities such as glycerol, free fatty acids, alcohol, and catalysts found in biodiesel enhance the corrosion rate [10]. Automotive engine parts made of metals such as cast iron, steel, copper alloys, and aluminium are susceptible to corrosion [11]. In this regard, corrosion study has become a crucial issue for the useability of biodiesel.

Therefore, researchers worldwide have focused on studying the corrosive nature of different biodiesels [12]. For example, the uses of vegetable [13], canola [14], sunflower [15], palm [16], and soybean [17] oil have been studied using different automotive materials. Rocabruno-Valdés et al. [13] compared the corrosion characteristics of pure copper, aluminium, stainless steel, and carbon steel in canola biodiesel using electrochemical methods for 528 h. It was observed that stainless steel is more susceptible to petting corrosion, while the corrosion rate of carbon steel is highest, whereas copper showed the lowest corrosion rate. Sorate et al. [7] investigated the corrosion characteristics of biodiesel with automotive materials such as copper, aluminium, leaded bronze, brass, and stainless steel using an immersion test. Results showed that the corrosion rate of copper is the highest, while that of stainless steel is the lowest. Similar studies [18,19] reported that copper and its alloy are more susceptible to corrosion among the fuel system materials than stainless steel and carbon steel.

Samuel et al. [15] characterised the corrosion behaviours of sunflower oil biodiesel and diesel in brass using a static immersion approach at room temperature. Results showed that the corrosion rate of brass exposed to 100% sunflower biodiesel is the highest, while the corrosion rate is lowest in diesel. Deshpande et al. [20] studied the corrosion characteristics of nodular cast iron used for making piston rings in palm biodiesel using a static immersion test for 30, 60, and 90 days. They found that the corrosion rate of 100% biodiesel is significantly higher than that of diesel. Moreover, it was found that the concentration of oxygen is higher in biodiesel due to fatty acids. A similar study [7] reported that biodiesel has maximum oxygen content and additional oxygen eventuated due to exposure to metals. This additional amount of oxygen retransforms esters into various acids such as acetic acid, formic acid, caproic acid, and propionic acid, which accelerate the corrosion rate in biodiesel.

From the above literature, it is evident that most of the studies focused on the corrosion characteristics of first-generation biodiesel. A limited number of studies are available regarding the corrosion characteristics of second-generation biodiesel [21,22]. Therefore, this present study investigates the corrosion characteristics of second-generation *Jatropha* biodiesel blends with the presence of commonly used automotive materials such as stainless steel, aluminium, copper, and cast iron using the immersion test method. These materials were chosen because they are exposed to fuel while passing from the fuel tank to the combustion chamber. For example, in the internal combustion engine, 100%, 19%, and 70% aluminium are used for manufacturing the piston, engine block, and cylinder head,

respectively [23]. Likewise, copper and its alloy are used to make pumps, injectors, and bearings [18,24]. Most parts such as nozzles, fuel filters, valves, and pump rings are made of stainless steel [24,25], while cast iron is used to make the liner [26].

## 2. Methodology

### 2.1. Material Preparation

This study studied the corrosion characteristics of commonly used automotive materials, such as stainless steel (17.14% Cr, 16.28% Ni, and 0.98% C), aluminium (95.73% pure), cast iron, and copper (95.37% pure) were analysed by the immersion test (IT) method [22]. The mechanical properties of the tested material samples are shown in Table 1. The samples were prepared from the round bar by machining, grinding, and polishing. The diameter of the material sample was 2.54 cm with a thickness of 4.0 mm. A 2.0 mm hole in each material sample was drilled to hang the coupons by Teflon wire in the fuel sample. The photographs of different metal samples are illustrated in Figure 1. Before exposing the metal sample into the fuel, it was treated as follows: polished with silicon carbide abrasive papers (from grade 400 to 1500), then washed and degreased with acetone. The samples were immersed into 10% H<sub>2</sub>SO<sub>4</sub> at room temperature for a few minutes; this was followed by washing with purified water. In addition, after the IT, metal specimens were scrubbed lightly in a stream of water with a polymer brush [22,25].

**Table 1.** Specifications of the tested immersion test sample.

Parameters	Stainless Steel (SS)	Cast Iron (CI)	Copper (Cu)	Aluminium (Al)
Density (kg/m <sup>3</sup> )	754	696	869	269
Brinell Hardness Number	216	159	83	104
Vickers Hardness Number	265	190	97	107
Hardness (MPa)	2599	1863	951	1049



**Figure 1.** Photograph of different metal samples ((a): Cu; (b): Al; (c): SS; (d): CI) after the immersion test.

### 2.2. Fuel Sample Preparation

The tested second-generation Jatropha biodiesel and fossil diesel were supplied by a local Malaysian company, Xtract Tech Sdn Bhd, and Hakita Engineering Sdn Bhd. Jatropha biodiesel fractions of 20% and 30% of were used in this study because numerous studies recommended that up to 20–30% biodiesel can be used in the IC engine without modification. Prior to conducting the immersion test, several properties of both biodiesel and diesel were measured using various apparatus. For the IT, fuel samples were heated at 80 °C and stirred at 250 rpm over 1600 h [22,25]. A Multiple Magnetic Hotplate Stirrer controlled the temperature and rotational speed with a temperature accuracy of  $\pm 0.3$  °C. The container of the fuel samples was made of glass. After the IT, the properties of the fuel samples were investigated further to measure the changes in properties due to corrosion. Table 2 represents the key characteristics of both diesel and biodiesel under as-received conditions.

**Table 2.** Characteristics of pure diesel and biodiesel blends.

Properties	Unit	B0	B20	B30	B100
Density	kg/m <sup>3</sup>	833	839	842	875
Acid value	mg KOH/g	0.15	0.24	0.29	0.50
FFA content	%	-	0.04	0.06	0.20
Water content	mg/kg	-	100	150	500
Kinematic viscosity at 40 °C	mm <sup>2</sup> /s	3.63	3.78	3.88	4.71
Flash point	°C	68	89	107	202
Induction period	h	106	85	75	3.02
Heating value	(MJ/kg)	45.5	44.3	43.7	39.5

### 2.3. Corrosion Rate Calculation

The average weight loss of the metal samples was calculated using samples measured before and after exposure to fuels at elevated temperatures. At the end of the test, the extent of corrosion was investigated by corrosion rate measurements and changes in surface morphology. The obtained data from weight loss were converted into corrosion rate (m/y) using Equation (1) [27].

$$\text{Corrosion rate (m/y)} = \frac{w \times 3.45 \times 10^6}{d \times t \times a} \quad (1)$$

where the corrosion rate is in mils per year,  $w$  is the weight loss of the samples,  $d$  is the density of the materials,  $t$  is exposure time and,  $a$  is the exposed surface area.

### 2.4. Surface Morphology Analysis

After the immersion tests, the corroded surface, pit morphology, and microstructure were studied by optical microscopy and scanning electron microscopy (SEM) with energy-dispersive X-ray spectroscopy (EDS). In this study, a Hitachi S-4700 FE-SEM was used to analyse the surface morphology using secondary electron mode at different magnifications. However, only the images with 1000× magnifications are reported in this study. Before inserting into the machine, all samples, including the holder were dried and cleaned carefully. The elemental composition of the specimens was examined using the EDS facility of the instrument before and after the immersion test.

### 2.5. Fuel Characterisation after Immersion Test

After the immersion test, the properties of biodiesel, such as density, viscosity, oxidation stability, total acid number (TAN), and water content, were investigated and compared with the diesel. The density and kinematic viscosity were measured by Anton Paar SVM-3000 using ASTM D341 and ASTM D445 standards. A 737 KF coulometer measured water content.

## 3. Results and Discussion

### 3.1. Corrosive Wears Analysis

Figure 2 shows the comparative corrosion rate (m/y) of different materials (SS, Al, Cl, and Cu). The highest corrosion rate is observed for Cu, whereas the lowest is observed for stainless steel using both biodiesel and diesel. Noticeably, the rate of corrosion in biodiesel is much higher than in diesel. The corrosion in engine parts made of metals, alloys, and elastomers with the presence of biodiesel occurs due to the chemical composition of biodiesel, consisting of unsaturated free fatty that easily undergoes oxidation. The performance and durability of IC engines fueled with biodiesel are largely influenced by oxygen in the functional groups (moieties), free fatty acids, degree of unsaturation, and hygroscopic nature of the biodiesel [28].

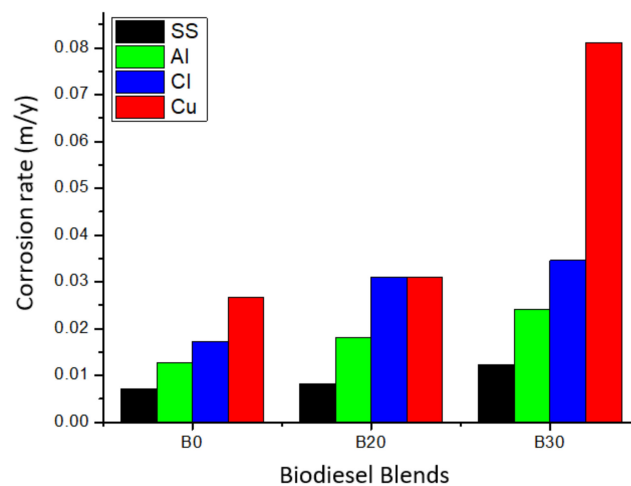


**Figure 2.** The comparative corrosion rate of different materials using the immersion test at 80 °C for 1600 h.

As seen, copper is more susceptible to corrosion than all other materials due to the highest weight loss [19,28]. The corrosion of SS is found to be the least. Steel is an alloy comprised mostly of iron and has a carbon content of 0.98% by weight. The carbon content in the steel might be a reason for its high resistance to corrosion [29]. The corrosion rate of Cu, CI, Al, and SS is determined to be 0.031, 0.031, 0.018, and 0.009 m/y in B20, while it is 0.81, 0.035, 0.025, and 0.012 m/y in B30. The corrosion rates of those materials are significantly lower in diesel, with a value of 0.026, 0.017, 0.012, and 0.0067 m/y using Cu, CI, Al, and SS. Kaul et al. [30] investigated the corrosion behaviour of piston (aluminium/aluminium alloy) and piston liner metal (cast iron/ferrous alloy) using a static immersion test for 7200 h at ambient temperature in diesel and several biodiesels such as *Jatropha curcas*, *kranja*, *mahua* oil, and *salvadora*. The investigation result revealed that the corrosion rate of piston metal (aluminium) in *Jatropha curcas*, *Mahua*, *Karanja*, and diesel are almost similar. The corrosion rate of *Jatropha curcas* biodiesel in the current study is about four times lower than the study conducted by Kaul et al. [30]. In addition, Kaul et al. [30] found the corrosion rate of 0.0784 m/y for cast iron, which is 2.5 times higher than that of the current study using B20 and 2.2 times higher using B30. According to the present study, the corrosion rate of cast iron (0.032 m/y) is lower than aluminium (0.018 m/y) in the case of B20. In addition, the corrosion rate of cast iron (0.035 m/y) is lower than aluminium (0.023 m/y) using B30. The variation in corrosion rate is due to the difference in material composition between the two metal alloys. Kaul et al. [30] reported that cast iron is more prone to corrosion than aluminium. The rate of corrosion largely depends on the fatty acid composition present in the biodiesel. Higher unsaturated fatty acid concentration with longer chain carbon–carbon double bonds has more prone to oxidise, which leads to a higher rate of corrosion [31].

Fazal et al. [25] investigated the corrosion rate of 99% pure copper, pure aluminium, and 316 stainless steel in palm biodiesel using an immersion test at a temperature of 80 °C with a stirring speed of 250 and duration of 1200 h. Results showed that the corrosion rates for copper, aluminium, and stainless steel are 0.586, 0.202, and 0.015 m/y, respectively, which are over five times higher than that of the current study using copper and aluminium, while they are similar with stainless steel with the presence of *Jatropha* biodiesel. The comparative results of the corrosion rate demonstrate that *Jatropha curcas* biodiesel is less corrosive than palm and *Salvadora* biodiesels, while it is slightly more corrosive than *Karanja* and *mahua* biodiesels [25,30]. However, it is to be noted that the corrosion rate for different biodiesels is affected by the experimental conditions, including temperature, light, relative humidity, rotational speed, and material and fuel sample compositions [32,33]. Referring to Figure 2, the higher the blend concentration, the higher the corrosion rate for

all materials. For example, the corrosion rate of copper in B0 is 0.0264 m/y, which is 0.031 in B20 (17% higher than B0); and 0.081 in B30 (206% higher than B0). However, depending on the materials, the rate was varied significantly. The higher corrosion rate using higher biodiesel blends is due to the higher unsaturated fatty acid content, total acid value, and strong affinity to attract and hold water content.

### 3.2. Surface Morphology Analysis

Figure 3 represents the optical micrograph of the Cu, CI, Al, and SS after the immersion test at 80 °C for 1600 h using both biodiesel and diesel. As seen, Cu and CI are highly susceptible to corrosions; this is followed by Al and SS concerning blend concentration.

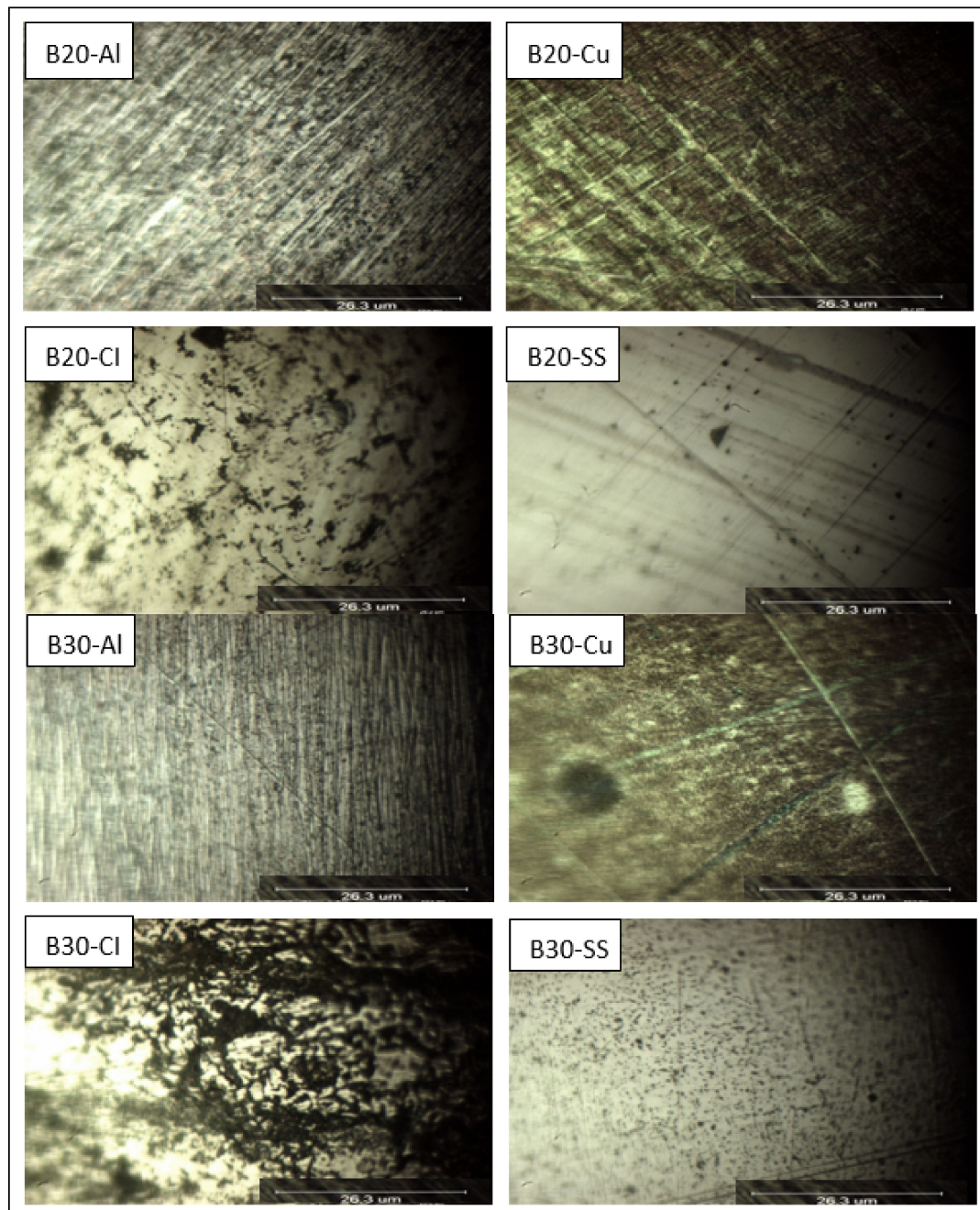


Figure 3. Optical micrograph (magnification: 500×) of different materials after the immersion test immersed into biodiesel.

There are several steps for pitting corrosion, starting from passive film breakdown to metastable pitting and finally pit growth. The material composition [34] and temperature [35] are two common factors affecting materials' pit growth. Szklarska-Smialowska [36] reported four stages of pitting corrosion, including (i) processes occurring at the boundary of the passive film and the solution; (ii) processes occurring within the passive film when no visible microscopic changes occur in a film; (iii) the formation of so-called metastable pits that initiate and grow for a short period below the critical pitting potential; and then re-passivation and (iv) stable pit growth. It is widely documented that microorganisms tend to attach themselves to surfaces, colonise, proliferate, and form a biofilm. The biofilm, consisting of microbial cells and their metabolic products, including extracellular polymeric substance (EPS), creates gradients of pH, leading to the corrosion of materials and alloys with the presence of biodiesels [37–39]. These corrosion processes refer to the biocorrosion or microbiologically influenced corrosion of materials [40,41].

After the immersion test, tarnishing, pitting, and cracking of the metal samples' worn surfaces were investigated by scanning electron microscopy (SEM). The microstructure of as-received and post-immersion test samples with a magnification of  $1000\times$  is shown in Figure 4. It is observed that the surfaces of the metal coupons immersed into biodiesel have pitted more compared to that of diesel. In addition, while comparing different materials, the Cu and CI surfaces corroded more than the other two materials. The size and distribution of the pits also varied with respect to the relative ionic concentration of the specimen [25]. At elevated temperature, a film of  $\text{CuO}/\text{CuCO}_3$  (outer layer) was formed on the surface of the Cu, followed by a layer of  $\text{Cu}_2\text{O}$  (inner layer) with the presence of  $\text{O}_2$  [42]. Whereas, at a higher temperature and oxygenated atmosphere, the aluminium surface formed a layer of  $\text{Al}_2\text{O}_3$  stronger than those formed on the copper surface. Thereby, copper is affected more by corrosion than aluminium. Furthermore, passivation on the aluminium surface significantly protects the corrosion constituents of the fuels [43]. An insignificant change in SS has appeared with respect to increasing blend concentrations.

The results from the elemental analysis of copper, aluminium, cast iron, and stainless-steel surfaces upon exposure to B20 biodiesel are presented in Figure 5.

It is found that the formation of the oxide layer may occur by replacing the metal outward or oxygen inward [44]. Consequently, the main compounds of the test samples Cu, Al, and Fe have reduced considerably after the immersion test. However, the changes are minimal for SS. Carbon and oxygen elements detected on the surface of the materials are present because of the formation of an oxide layer using biodiesel. Due to corrosion, there was damage on the surfaces of the materials, which led to significantly increased carbon content for all materials. The increase in carbon content was due to the organic deposits, including oxide layers or fatty acid salts.

### 3.3. Change in Fuel Composition after the Immersion Test

Figure 6 shows the appearance of diesel and biodiesels samples as received and post-immersion test using different materials. As seen, as-received diesel and biodiesel samples are clear and yellowish. As noticed, as the blend concentration increases, the appearance becomes more yellowish and denser. After the immersion test, the diesel and biodiesel samples' colour changed dramatically due to the corrosion product. The changes in the colour of the fuel sample reflect the formation of the oxide film in copper-immersed samples. The change in colour in the biodiesel sample results from the formation of  $\text{Al}_2\text{O}_3$  and  $\text{CuCO}_3$  using Al and Cu-immersed samples [45,46]. The red colour of diesel (B0) is likely due to the presence of  $\text{Cu}_2\text{O}$ .

The major acidic compounds in Jatropha biodiesel are oleic, linoleic, palmitic, and stearic acids [22,47]. After the immersion test, palmitic, stearic and oleic acids were increased, which led to decrease in the biodiesel properties and increased corrosion rate [48]. The oxidation products of the materials immersed in fuel react with the free fatty acid of the biodiesel and form fatty acid salt on the surface of the metal sample, which further enhances the corrosion rate on the surface of the metal. For example,  $\text{CuO}$  and  $\text{Fe}_2\text{O}_3$  play a

significant role in the oxidation of biodiesel. The reaction between the ester compound and the oxygen present in the biodiesel produces some chemical compounds such as aldehyde and ketones, which also change the colour of the fuel samples [49].

### 3.4. Fuel Properties after Immersion Test

After the immersion test, the change in viscosity for the fuel samples is shown in Figure 7. The viscosity after the test is increased for diesel and biodiesel, although the increment in biodiesel is markedly higher than diesel. This phenomenon can be explained as the difference in the composition of the fuels since diesel fuel consists of hundreds of different compounds, while biodiesel usually contains only four to five major compounds that all boil at about the same temperature [50]. Therefore, when these two different types of fuels (diesel and biodiesel) are blended and stored at temperature for a certain period, there are some chemical compositional changes in the blends. In addition, the molecular structure of biodiesel changes more robustly than that of pure diesel.

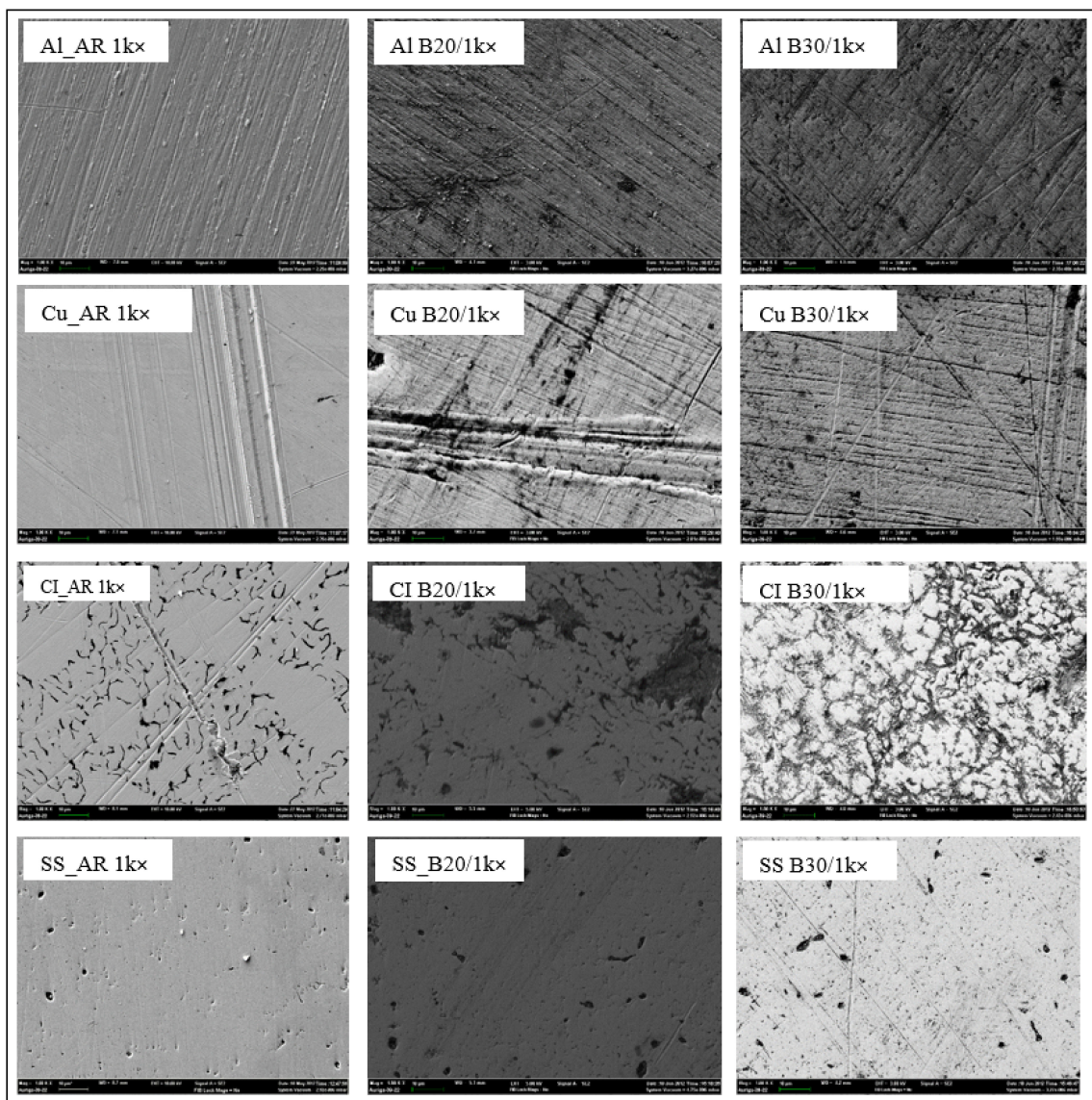


**Figure 4.** SEM microstructure of different materials immersed into biodiesel as received (AR) and post-immersion test samples.

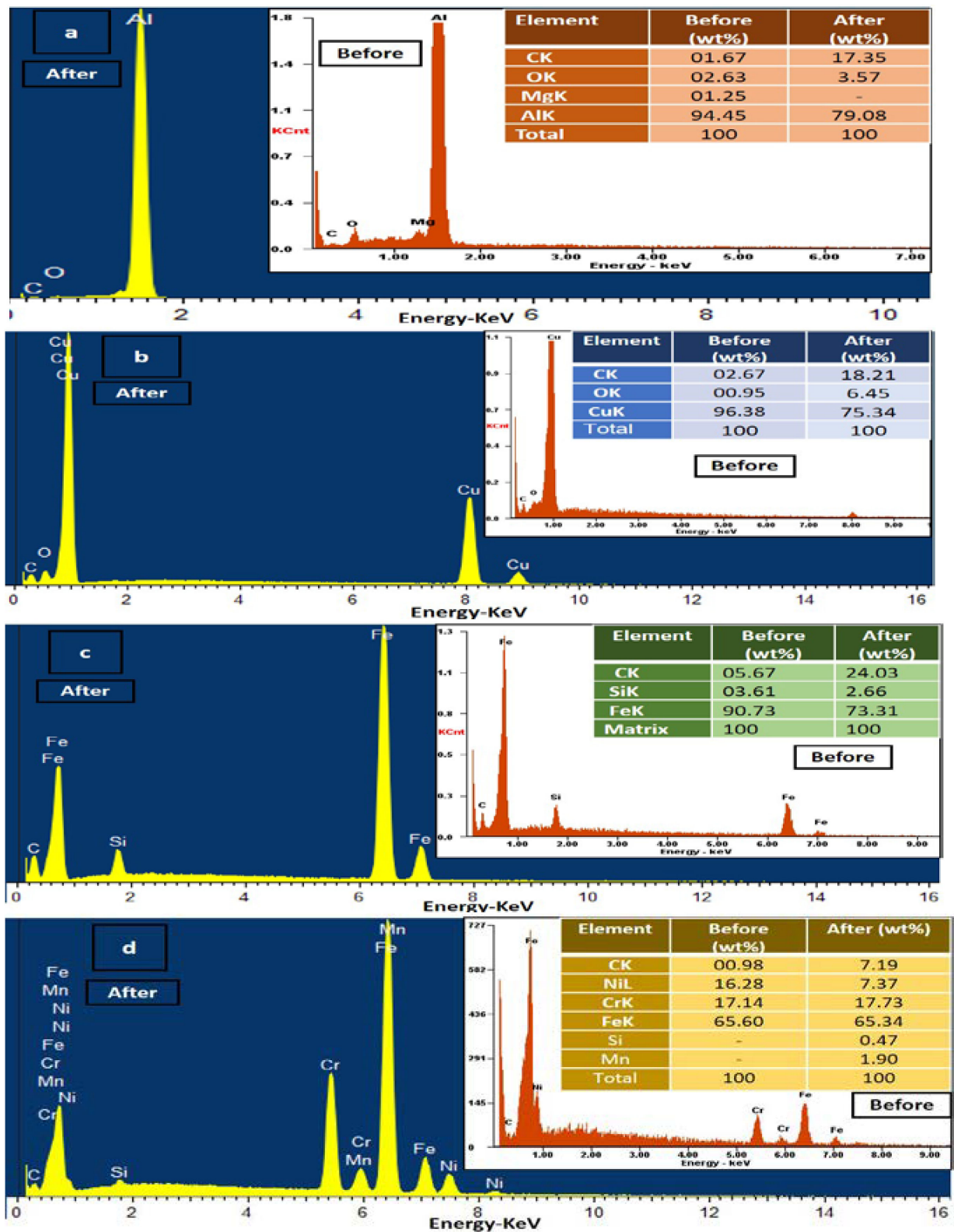


**Figure 5.** Elemental analysis of different materials immersed into B20 after the immersion test: (a) Al, (b) Cu, (c) CI, and (d) SS.

The viscosity of diesel in the as-received condition was 3.5 mm<sup>2</sup>/s, which increased to 6.9, 5.0, 4.4, and 4.2 mm<sup>2</sup>/s for CI, Cu, SS, and Al immersed fuels. In contrast, in the

as-received condition, the viscosity of B20 and B30 was 3.8 and 3.9 mm<sup>2</sup>/s, which increased to 7.0–12.0 mm<sup>2</sup>/s after the immersion test using different materials. According to the standard limit for viscosity set by ASTM D6751, none of the biodiesel samples maintain a standard viscosity limit of 6.0 mm<sup>2</sup>/s after the immersion test. A large fluctuation in viscosity for B20 and B30 was found concerning the materials exposed. In most of the cases, cast-iron immersed biodiesel showed the maximum viscosity change (more than 12 mm<sup>2</sup>/s for both B20 and B30), while an aluminium immersed biodiesel showed the least increment (<6.7 mm<sup>2</sup>/s for B20 and B30).

Figure 8 shows the changes in density after the immersion test for both biodiesel and diesel. After the immersion test, the density of the samples using diesel is nearly similar, with  $\approx 830$  kg/m<sup>3</sup>. Whereas for B20, the density of the samples fluctuated between 835 (Al immersed fuel) and 870 kg/m<sup>3</sup> (CI immersed fuel). For B30, the density of samples fluctuated between 850 (Al immersed fuel) and 870 kg/m<sup>3</sup> (SS immersed fuel). However, all samples satisfy the standard density limit set by ASTM D975 and ASTM D 6751 for diesel and biodiesel.

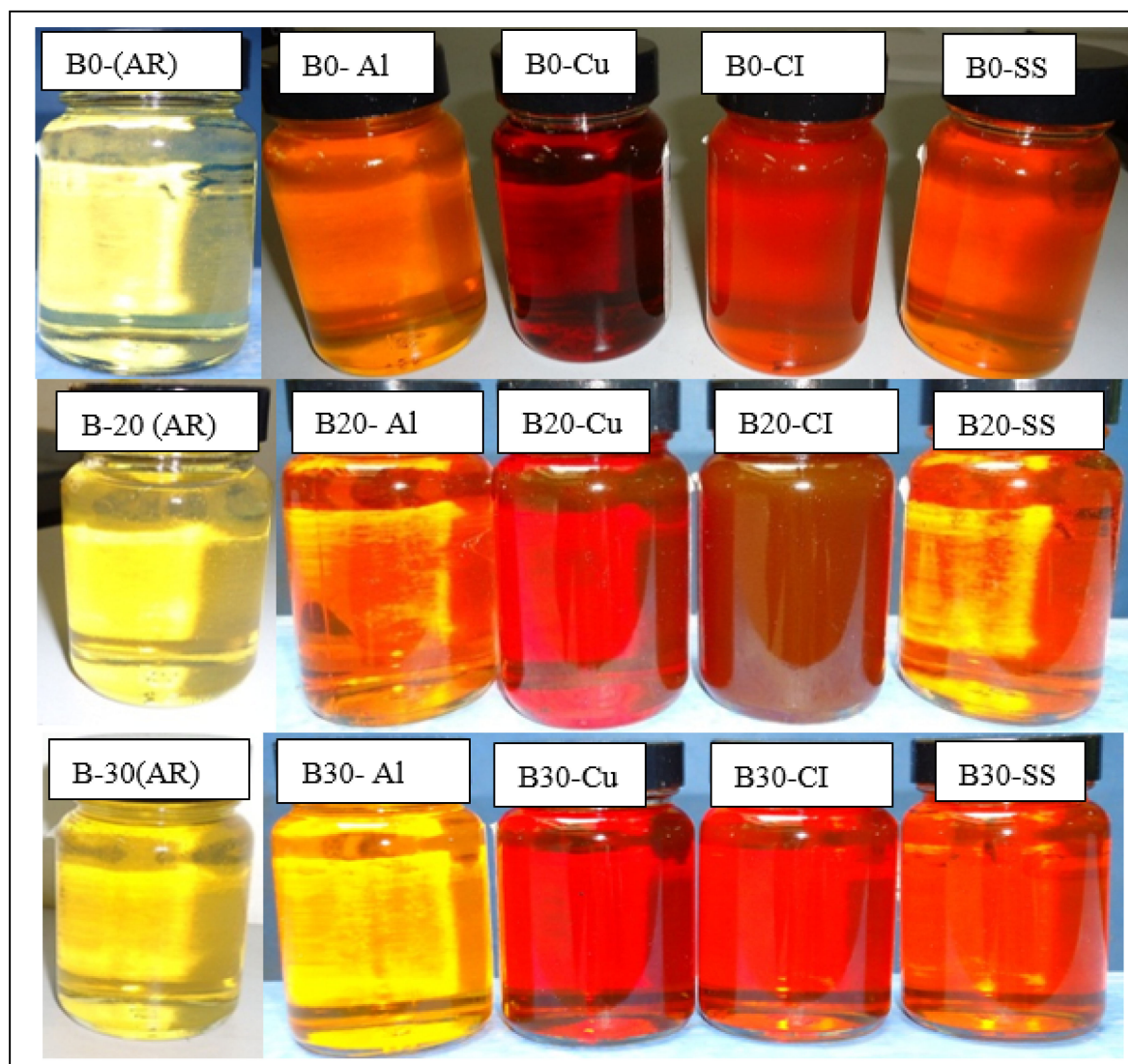


**Figure 6.** The appearance of biodiesel and diesel after the immersion for 1600 h.

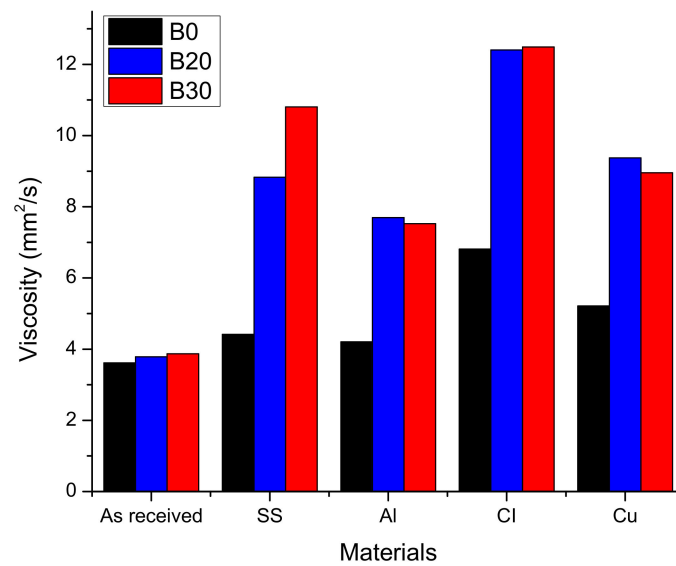


Figure 7. Change in viscosity of biodiesel after the immersion test with different materials.

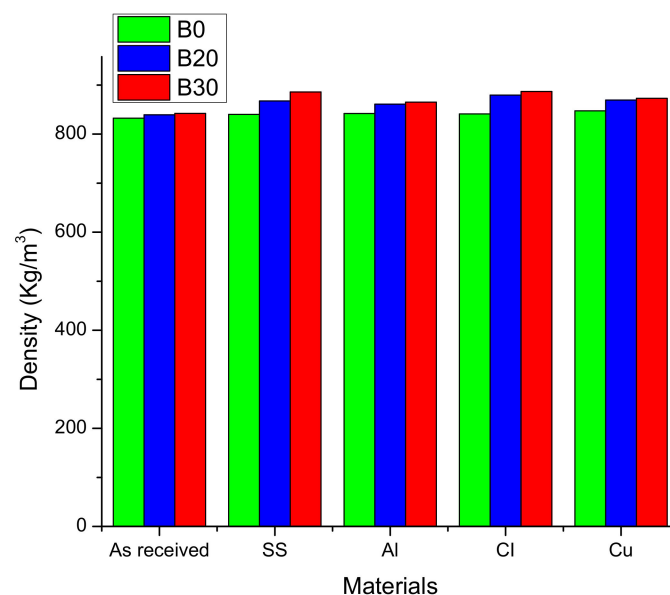
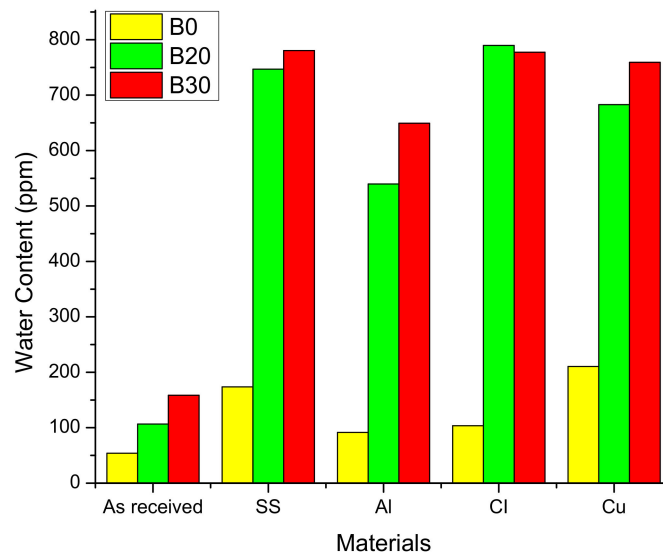


Figure 8. Change in the density of biodiesel after the immersion test with different materials.

According to Figure 9, the water content increases significantly, especially for biodiesel. B0 contained water content of 50 ppm in the as-received condition, which increased to 175 ppm for SS, 88 ppm for Al, 100 ppm for CI, and 200 ppm for Cu immersed fuel. The water content increased to 550–790 ppm using different material immersed biodiesels from as-received 105 (B20) and 155 (B30) ppm. Due to the hygroscopic nature of the biodiesel, more water content was absorbed by the samples, which led to an increase in the corrosion rate. Microbial growth increases due to the higher water content in the fuel, leading to an increase in the corrosion rate [51]. In addition, water, particularly at a higher temperature, can hydrolyse esters and triglycerides and produce different fatty acids, which are more corrosive [52]. However, all fuel samples maintain the standard limit (ASTM D 6751) for water content.



**Figure 9.** Change in water content of biodiesel after the immersion test with different materials.

The TAN property of biodiesel plays a significant role to enhance the corrosion rate. The higher TAN value leads to an increase in the oxidation process in material-immersed fuels. Figure 10 illustrates the change in TAN value for both biodiesel and diesel after the immersion test. As observed, the rate of increment in TAN value for diesel was not too significant; however, a considerable increase in the TAN value is seen for biodiesel. After the immersion test, Cu and CI immersed in B0 showed a maximum value of 0.36 mgKOH/g, while Al and SS immersed in B0 showed the TAN value of 0.3 and 0.25 mgKOH/g, respectively.

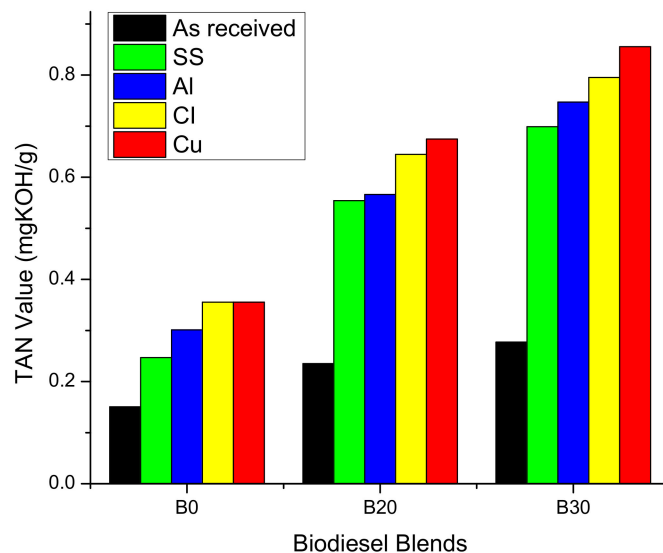


**Figure 10.** Change in TAN value of biodiesel after the immersion test with different materials.

The TAN value for B20 and B30 was also increased for all samples. Cu-immersed fuel imparts the highest TAN value for all fuel samples, followed by CI, Al, and SS-immersed fuels. The study conducted by Kaul et al. [30] using the static immersion test found a significant increment in TAN value using Al and CI-immersed biodiesels including *Jatropha curcas*, *Karanja*, *Mahua*, and *Salvadora*. Due to the oxidation in biodiesel, the TAN value of the fuel increases [53].

Table 3 represents the oxidation stability of fuel samples under as-received and after

immersion test conditions. It is depicted that the oxidation stability of both biodiesel and diesel decreases after the immersion test dramatically. In the as-received condition, the induction period (a measure of oxidation stability) of B0, B20, and B30 are 106, 85, and 75 h, respectively. However, after the immersion test of 1600 h, the induction period (IP) for Al, SS, Cu, and CI immersed B0 was 96, 42, 45, and 21 h, respectively. The oxidation stability of B20 and B30 has also decreased significantly with a value of 0.3–2.25 h from its initial 75–80 h. The result implies that biodiesel oxidises more robustly and is less stable than diesel. The results obtained in the current study are in good agreement with the results obtained by Hancsok et al. [54].

**Table 3.** Oxidation stability (induction period, h) of the fuel samples after the immersion test.

Metal Sample	As-Received Fuels (IP/h)			After the Immersion Test (IP/h)		
	B0	B20	B30	B0	B20	B30
SS	106	85	75	42	0.60	0.35
Al	106	85	75	96	0.75	0.30
Ci	106	85	75	21	2.25	0.32
Cu	106	85	75	45	0.60	0.50

#### 4. Conclusions

Corrosion characteristics of widely used automotive materials including copper, cast iron, aluminium, and stainless steel exposed to *Jatropha* biodiesel and diesel were investigated. It is found that biodiesel is more corrosive than diesel. Concerning the corrosion rate and morphological change, copper is most susceptible to corrosion, followed by cast iron, aluminium, and stainless steel. The degradation of fuel properties, such as viscosity, density, water content, TAN, and IP was significantly higher for biodiesel than for diesel. With different materials, biodiesel is oxidised more, resulting in the formation of various acids and therefore the increase in TAN value. A higher degradation of *Jatropha* biodiesel than diesel is due to unsaturated fatty acid, higher oxygen moieties, the hygroscopic nature, and the auto-oxidation properties of biodiesel. The degree of degradation concerning blend concentrations (B20 and B30) was insignificant concerning TAN and density. In contrast, the degree of degradation was noticeable in SS and Cu-immersed samples in terms of density, and Al and Cu-immersed samples in terms of water content. Although the difference in corrosion rate between B20 and B30 is not significant except for copper, it is recommended to limit *Jatropha* biodiesel up to 20% for an extended durability of fuel system parts.

**Author Contributions:** Conceptualization, M.S.; methodology, M.S.; software, M.B.A.S.; validation, M.S. and M.M.; formal analysis, M.S.; investigation, M.S.; resources, M.A.K. and H.H.M.; data curation, M.S.; writing—original draft preparation, M.S.; writing—review and editing, M.S. and M.A.K.C.; visualization, M.S. and M.M.; supervision, M.A.K. and H.H.M.; project administration, M.A.C.; funding acquisition, M.A.K. All authors have read and agreed to the published version of the manuscript.

**Funding:** This research was funded by Universiti Malaya, grant number FP142-2019A.

**Institutional Review Board Statement:** Not applicable.

**Informed Consent Statement:** Not applicable.

**Data Availability Statement:** Not applicable.

**Acknowledgments:** The authors would like to thank the Department of Mechanical Engineering, Universiti Malaya and FRGS research grant with Project no: FP142-2019A for the experimental and financial support.

**Conflicts of Interest:** The authors declare no conflict of interest.

## References

1. Baena, L.M.; Calderón, J.A. Effects of palm biodiesel and blends of biodiesel with organic acids on metals. *Heliyon* **2020**, *6*, e03735. [[CrossRef](#)]
2. Gavhane, R.; Kate, A.; Soudagar, M.E.M.; Wakchaure, V.; Balgude, S.; Rizwanul Fattah, I.; Nik-Ghazali, N.-N.; Fayaz, H.; Khan, T.; Mujtaba, M.; et al. Influence of silica nano-additives on performance and emission characteristics of Soybean biodiesel fuelled diesel engine. *Energies* **2021**, *14*, 1489. [[CrossRef](#)]
3. Mofijur, M.; Masjuki, H.H.; Kalam, M.A.; Atabani, A.E.; Fattah, I.M.R.; Mobarak, H.M. Comparative evaluation of performance and emission characteristics of Moringa oleifera and Palm oil based biodiesel in a diesel engine. *Ind. Crop. Prod.* **2014**, *53*, 78–84. [[CrossRef](#)]
4. Mofijur, M.; Atabani, A.E.; Masjuki, H.H.; Kalam, M.A.; Masum, B.M. A study on the effects of promising edible and non-edible biodiesel feedstocks on engine performance and emissions production: A comparative evaluation. *Renew. Sustain. Energy Rev.* **2013**, *23*, 391–404. [[CrossRef](#)]
5. Mahlia, T.M.I.; Syazmi, Z.A.H.S.; Mofijur, M.; Abas, A.E.P.; Bilad, M.R.; Ong, H.C.; Silitonga, A.S. Patent landscape review on biodiesel production: Technology updates. *Renew. Sustain. Energy Rev.* **2020**, *118*, 109526. [[CrossRef](#)]
6. Shahabuddin, M.; Masjuki, H.H.; Kalam, M.A.; Bhuiya, M.M.K.; Mehat, H. Comparative tribological investigation of bio-lubricant formulated from a non-edible oil source (Jatropha oil). *Ind. Crop. Prod.* **2013**, *47*, 323–330. [[CrossRef](#)]
7. Sorate, K.A.; Bhale, P.V. Biodiesel properties and automotive system compatibility issues. *Renew. Sustain. Energy Rev.* **2015**, *41*, 777–798. [[CrossRef](#)]
8. Shahabuddin, M.; Liaquat, A.; Masjuki, H.; Kalam, M.; Mofijur, M. Ignition delay, combustion and emission characteristics of diesel engine fueled with biodiesel. *Renew. Sustain. Energy Rev.* **2013**, *21*, 623–632. [[CrossRef](#)]
9. Hoang, A.T.; Tabatabaei, M.; Aghbashlo, M. A review of the effect of biodiesel on the corrosion behavior of metals/alloys in diesel engines. *Energy Sources Part A Recovery Util. Environ. Eff.* **2020**, *42*, 2923–2943. [[CrossRef](#)]
10. Singh, B.; Korstad, J.; Sharma, Y.C. A critical review on corrosion of compression ignition (CI) engine parts by biodiesel and biodiesel blends and its inhibition. *Renew. Sustain. Energy Rev.* **2012**, *16*, 3401–3408. [[CrossRef](#)]
11. Fazal, M.A.; Jakeria, M.R.; Haseeb, A.S.M.A.; Rubaiee, S. Effect of antioxidants on the stability and corrosiveness of palm biodiesel upon exposure of different metals. *Energy* **2017**, *135*, 220–226. [[CrossRef](#)]
12. Fazal, M.A.; Rubaiee, S.; Al-Zahrani, A. Overview of the interactions between automotive materials and biodiesel obtained from different feedstocks. *Fuel Process. Technol.* **2019**, *196*, 106178. [[CrossRef](#)]
13. Rocabrundo-Valdés, C.I.; Hernández, J.A.; Juantorena, A.U.; Arenas, E.G.; Lopez-Sesenes, R.; Salinas-Bravo, V.M.; González-Rodríguez, J.G. An electrochemical study of the corrosion behaviour of metals in canola biodiesel. *Corros. Eng. Sci. Technol.* **2018**, *53*, 153–162. [[CrossRef](#)]
14. Sorate, K.A.; Bhale, P.V. Corrosion Behavior of Automotive Materials with Biodiesel a Different Approach. *SAE Int. J. Fuels Lubr.* **2018**, *11*, 147–162. [[CrossRef](#)]
15. Samuel, O.D.; Gulum, M. Mechanical and corrosion properties of brass exposed to waste sunflower oil biodiesel-diesel fuel blends. *Chem. Eng. Commun.* **2019**, *206*, 682–694. [[CrossRef](#)]
16. Amaya, A.; Piamba, O.; Olaya, J. Corrosiveness of Palm Biodiesel in Gray Cast Iron Coated by Thermoreactive Diffusion Vanadium Carbide (VC) Coating. *Coatings* **2019**, *9*, 135. [[CrossRef](#)]
17. Deyab, M.A.; Corrêa, R.G.C.; Mazzetto, S.E.; Dhmees, A.S.; Mele, G. Improving the sustainability of biodiesel by controlling the corrosive effects of soybean biodiesel on aluminum alloy 5052 H32 via cardanol. *Ind. Crop. Prod.* **2019**, *130*, 146–150. [[CrossRef](#)]
18. Fraer, R.; Dinh, H.; Proc, K.; McCormick, R.L.; Chandler, K.; Buchholz, B. Operating Experience and Teardown Analysis for Engines Operated on Biodiesel Blends. In Proceedings of the 2005 SAE Commercial Vehicle Engineering Conference, Rosemont, IL, USA, 1–3 November 2005.
19. Geller, D.P.; Adams, T.T.; Goodrum, J.W.; Pendergrass, J. Storage stability of poultry fat and diesel fuel mixtures: Specific gravity and viscosity. *Fuel* **2008**, *87*, 92–102. [[CrossRef](#)]
20. Deshpande, S.; Joshi, A.; Vagge, S.; Anekar, N. Corrosion behavior of nodular cast iron in biodiesel blends. *Eng. Fail. Anal.* **2019**, *105*, 1319–1327. [[CrossRef](#)]
21. Fazal, M.A.; Suhaila, N.R.; Haseeb, A.S.M.A.; Rubaiee, S. Sustainability of additive-doped biodiesel: Analysis of its aggressiveness toward metal corrosion. *J. Clean. Prod.* **2018**, *181*, 508–516. [[CrossRef](#)]
22. Ahmmad, M.S.; Haji Hassan, M.B.; Kalam, M.A. Comparative corrosion characteristics of automotive materials in Jatropha biodiesel. *Int. J. Green Energy* **2018**, *15*, 393–399. [[CrossRef](#)]
23. Cole, G.; Sherman, A. Light weight materials for automotive applications. *Mater. Charact.* **1995**, *35*, 3–9. [[CrossRef](#)]
24. Sgroi, M.; Bollito, G.; Saracco, G.; Specchia, S. BIOFEAT: Biodiesel fuel processor for a vehicle fuel cell auxiliary power unit: Study of the feed system. *J. Power Sources* **2005**, *149*, 8–14. [[CrossRef](#)]
25. Fazal, M.; Haseeb, A.; Masjuki, H. Comparative corrosive characteristics of petroleum diesel and palm biodiesel for automotive materials. *Fuel Process. Technol.* **2010**, *91*, 1308–1315. [[CrossRef](#)]
26. Fazal, M.A.; Haseeb, A.S.M.A.; Masjuki, H.H. Effect of different corrosion inhibitors on the corrosion of cast iron in palm biodiesel. *Fuel Process. Technol.* **2011**, *92*, 2154–2159. [[CrossRef](#)]
27. Fontana, M.G. *Corrosion Engineering*, 3rd ed.; McGraw-Hill: New York, NY, USA, 1986.

28. Fazal, M.A.; Haseeb, A.S.M.A.; Masjuki, H.H. Biodiesel feasibility study: An evaluation of material compatibility; performance; emission and engine durability. *Renew. Sustain. Energy Rev.* **2011**, *15*, 1314–1324. [[CrossRef](#)]
29. Cao, P.; Tremblay, A.Y.; Dube, M.A.; Morse, K. Effect of membrane pore size on the performance of a membrane reactor for biodiesel production. *Ind. Eng. Chem. Res.* **2007**, *46*, 52–58. [[CrossRef](#)]
30. Kaul, S.; Saxena, R.; Kumar, A.; Negi, M.; Bhatnagar, A.; Goyal, H.; Gupta, A. Corrosion behavior of biodiesel from seed oils of Indian origin on diesel engine parts. *Fuel Process. Technol.* **2007**, *88*, 303–307. [[CrossRef](#)]
31. Shahabuddin, M.; Kalam, M.A.; Masjuki, H.H.; Bhuiya, M.M.K.; Mofijur, M. An experimental investigation into biodiesel stability by means of oxidation and property determination. *Energy* **2012**, *44*, 616–622. [[CrossRef](#)]
32. Wood, R.; Hutton, S.; Schiffrin, D. Mass transfer effects of non-cavitating seawater on the corrosion of Cu and 70Cu-30Ni. *Corros. Sci.* **1990**, *30*, 1177–1201. [[CrossRef](#)]
33. Keera, S.T.; Elham, E.A.; Taman, A.R. Corrosion of copper metal in distillation process. *Anti Corros. Methods Mater.* **1998**, *45*, 252–255. [[CrossRef](#)]
34. Frankel, G. Pitting corrosion of metals a review of the critical factors. *J. Electrochem. Soc.* **1998**, *145*, 2186–2198. [[CrossRef](#)]
35. Arnvig, P.E.; Davison, R.M. Corrosion Control for Low-Cost Reliability. In Proceedings of the 12th International Corrosion Congress, Houston, TX, USA, 19–24 September 1993; p. 1477.
36. Szklarska-Smialowska, Z. Pitting corrosion of aluminum. *Corros. Sci.* **1999**, *41*, 1743–1767. [[CrossRef](#)]
37. Liao, J.; Fukui, H.; Urakami, T.; Morisaki, H. Effect of biofilm on ennoblement and localized corrosion of stainless steel in fresh dam-water. *Corros. Sci.* **2010**, *52*, 1393–1403. [[CrossRef](#)]
38. Lee, W.; Beer, D. Oxygen and pH micro profiles above corrosion mild steel covered with a biofilm. *Biofouling* **1995**, *8*, 273–280. [[CrossRef](#)]
39. Street, C.N.; Gibbs, A. Eradication of the corrosion-causing bacterial strains *Desulfovibrio vulgaris* and *Desulfovibrio desulfuricans* in planktonic and biofilm form using photo disinfection. *Corros. Sci.* **2010**, *52*, 1447–1452. [[CrossRef](#)]
40. Beale, D.J.; Dunn, M.S.; Marney, D. Application of GC-MS metabolic profiling to blue-green water from microbial influenced corrosion in copper pipes. *Corros. Sci.* **2010**, *52*, 3140–3145. [[CrossRef](#)]
41. Sherar, B.W.A.; Power, I.M.; Keech, P.G.; Mitlin, S.; Southam, G.; Shoesmith, D.W. Characterizing the effect of carbon steel exposure in sulfide containing solutions to microbially induced corrosion. *Corros. Sci.* **2011**, *53*, 955–960. [[CrossRef](#)]
42. Mankowski, G.; Duthil, J.P.; Giusti, A. The pit morphology on copper in chloride- and sulphate-containing solutions. *Corros. Sci.* **1997**, *39*, 27–42. [[CrossRef](#)]
43. Norouzi, S.; Eslami, F.; Wyszynski, M.L.; Tsolakis, A. Corrosion effects of RME in blends with ULSD on aluminium and copper. *Fuel Process. Technol.* **2012**, *104*, 204–210. [[CrossRef](#)]
44. Evans, U.R. *The Corrosion and Oxidation of Metals: Scientific Principles and Practical Applications*, 1st ed.; Edward Arnold: London, UK, 1960.
45. Haseeb, A.S.M.A.; Masjuki, H.H.; Ann, L.J.; Fazal, M.A. Corrosion characteristics of copper and leaded bronze in palm biodiesel. *Fuel Process. Technol.* **2010**, *91*, 329–334. [[CrossRef](#)]
46. Huang, T.J.; Tsai, D.H. CO oxidation behavior of copper and copper oxides. *Catal. Lett.* **2003**, *87*, 173–178. [[CrossRef](#)]
47. Mofijur, M.; Masjuki, H.; Kalam, M.; Hazrat, M.; Liaquat, A.; Shahabuddin, M.; Varman, M. Prospects of biodiesel from Jatropa in Malaysia. *Renew. Sustain. Energy Rev.* **2012**, *16*, 5007–5020. [[CrossRef](#)]
48. Hu, E.; Xu, Y.; Hu, X.; Pan, L.; Jiang, S. Corrosion behaviors of metals in biodiesel from rapeseed oil and methanol. *Renew. Energy* **2012**, *37*, 371–378. [[CrossRef](#)]
49. Wagner, H.; Luther, R.; Mang, T. Lubricant base fluids based on renewable raw materials: Their catalytic manufacture and modification. *Appl. Catal. A Gen.* **2001**, *221*, 429–442. [[CrossRef](#)]
50. Wagutu, A.; Chhabra, S.; Thoruwa, C.; Thoruwa, T.; Mahunnah, R. Indigenous oil crops as a source for production of biodiesel in Kenya. *Bull. Chem. Soc. Ethiop.* **2009**, *23*, 47660. [[CrossRef](#)]
51. Kaminski, J.; Kurzydowski, K.J. Use of impedance spectroscopy on testing corrosion resistance of carbon steel and stainless steel in water-biodiesel configuration. *J. Corros. Meas.* **2008**, *6*, 1–5.
52. Thomas, E.W.; Fuller, R.E.; Terauchi, K. Fluoroelastomer Compatibility with Biodiesel Fuels. In Proceedings of the Commercial Vehicle Engineering Congress & Exhibition Powertrain & Fluid Systems Conference and Exhibition, Rosemont, IL, USA, 29 October–1 November 2007.
53. Tsuchiya, T.; Shiotani, H.; Goto, S.; Sugiyama, G.; Maeda, A. Japanese Standards for Diesel Fuel Containing 5% FAME Blended Diesel Fuels and its Impact on Corrosion. In Proceedings of the Powertrain & Fluid Systems Conference and Exhibition, Toronto, ON, Canada, 12–16 October 2006.
54. Hancsók, J.; Bubálik, M.; Beck, Á.; Baladincz, J. Development of multifunctional additives based on vegetable oils for high quality diesel and biodiesel. *Chem. Eng. Res. Des.* **2008**, *86*, 793–799. [[CrossRef](#)]